

## A Spectral Atlas of the Pre-WN Candidate HD 326823

Marcelo Borges Fernandes

borges@dag0.on.br

Francisco Xavier de Araújo

araujo@on.br

Claudio Bastos Pereira

claudio@on.br

Sayd J. Codina Landaberry

sayd@on.br

Observatório Nacional, Rua General José Cristino 77

CEP 20921-400, Rio de Janeiro BRAZIL

Received \_\_\_\_\_; accepted \_\_\_\_\_

---

<sup>1</sup>Based on observations mainly done with the 1.52m telescope at the European Southern Observatory (La Silla, Chile), under the agreement with the Observatório Nacional-MCT (Brazil) and also with the 1.6m telescope at the Laboratório Nacional de Astrofísica (Brasópolis, Brazil).

## ABSTRACT

HD 326823 is a peculiar emission line object. In the literature it was considered as a pre-WN candidate. Based mainly on high resolution data, obtained with the FEROS spectrograph, we made an atlas covering 3800-9200 Å region. This atlas confirms the presence of several strong HeI lines and numerous N lines. There is also a deficiency of H, indicating that this object is indeed in an evolved stage. In addition, with low resolution spectra, we obtained intensities of several lines.

*Subject headings:* stars: HD 326823 — stars: transition objects — Lines: identifications, intensities, equivalent widths

## 1. Introduction

The evolution of massive stars ( $M_{ZAMS} > 10 M_{\odot}$ ) is not yet completely understood. We know that they start their lives as O or B types and finish them in supernova explosions. Phases like LBV, WN, WC and B[e]sg need a better comprehension. The existence of few objects in these classes is a problem. This problem becomes bigger for transition evolutionary phases due to even smaller number of members. The possibility that HD 326823 (Hen 3-1330) is an object in a transition phase is the main reason that motivated the present study.

HD 326823 ( $l^{II} = 344.3; b^{II} = -1.2$ ) belongs to an association of distant OB supergiants in the direction of the galactic center at a distance  $R \sim 2$  kpc (McGregor, Hyland, & Hillier 1988). Feast et al. (1961) labelled it as a peculiar emission object, with emission lines of H, He I, Fe II, Mg II and interstellar absorption lines of Ca II. Stephenson (1974) noted that the great strength of the He I emission could be attributed to He overabundance and H deficiency.

McGregor et al. (1988) found that the continuum was essentially flat in flux between 1 and  $2.5 \mu\text{m}$ , with several He I emission lines and a few weak H I emission lines present. They concluded that He overabundance in the envelope of this star would suggest that HD 326823 is becoming a WR star. In the UV, Shore et al. (1990) reported a B-type absorption spectrum consistent with a B1.5 spectral type. In addition, they found that the spectrum is similar to the one of LBV S128/LMC = R127.

Lopes, Daminieli, & de Freitas Pacheco (1992), based on Coudé data limited to few spectral regions, confirmed the result of Carlson & Henize (1979), finding complex He I profiles with a double structure. This structure indicates that the lines are probably formed in different circumstellar regions with rotation. The red Ca II triplet and the Fe II 9997 Å feature also showed similar two-peak profiles. The spectra of Lopes et al. (1992) also

showed rather strong N lines, indicating a possible overabundance of this element. They suggested that HD 326823 may be the precursor of a WN star.

Sterken et al. (1995) made a spectroscopic and photometric study and confirmed the very peculiar nature of the star. They also suggested that HD 326823 may be a LBV in a quiescent state, having had S Dor-type eruptions in the past, and that it is now possibly moving towards a WN configuration. On the other hand, Lamers et al. (1998) and de Winter & Pérez (1998) included it in the group of unclassified B[e] stars.

More recently Walborn & Fitzpatrick (2000) presented a digital atlas of 20 high-luminosity, peculiar OB spectra in the 3800-4900 Å range. They put HD 326823 in the group of “Iron Stars”, but they cited that it “has perhaps the most bizarre spectrum in this atlas”. Moreover they have emphasized “the extreme weakness of all its spectral features, including hydrogen, which must be very deficient”.

In order to contribute to a better comprehension of the evolutionary stage of HD 326823, we present in this paper a spectral atlas in the 3800-9200 Å wavelength range. This atlas is based mainly on high resolution data obtained with the FEROS spectrograph (Kaufer et al. 1999) attached to the 1.52m ESO telescope.

## 2. Observations & Reductions

High and low resolution observations were both obtained with the ESO 1.52m telescope in La Silla (Chile).

HD 326823 was observed in high resolution mode on 1999 June 24, with an exposure time of 1800 seconds, in order to present a detailed line list. These data were also used to deblend some features present in the low resolution spectra. The Fiber-fed Extended Range Optical Spectrograph (FEROS) is a bench-mounted Echelle spectrograph with the fibers

located at the Cassegrain focus with a spectral resolving power of  $R = 48\,000$  corresponding to 2.2 pixels of  $15\mu\text{m}$  and with a wavelength coverage from  $3600\text{\AA}$  to  $9200\text{\AA}$ . FEROS has a complete automatic on-line reduction. Equivalent widths have been measured using an IRAF task that computes the line area above the adopted continuum. The FEROS spectrum of HD 326823 of the present paper has, in the  $5500\text{\AA}$  region, a S/N ratio in the continuum of approximately 45.

Low resolution spectra of HD 326823 were taken using a Boller & Chivens spectrograph at the Cassegrain focus on 1998 March 14, 1998 July 12, and 2000 June 9. Spectra of five other similar objects, that are mentioned below, were also obtained on different dates. Table 1 shows the log of the observations. Two instrumental setups were employed. The first one made use of grating #23 with  $600\text{ l mm}^{-1}$ , providing a resolution of  $\sim 4.6\text{\AA}$  in the ranges  $3600\text{--}7400\text{\AA}$  and  $3800\text{--}8700\text{\AA}$ . The other one used grating #32 with  $2400\text{ l mm}^{-1}$ , providing a resolution of  $\sim 1.0\text{\AA}$ , in the range  $3060\text{--}4060\text{\AA}$ . The Cassegrain spectra (hereafter the data obtained with the Boller & Chivens spectrograph will be denoted as Cassegrain data) were reduced using standard IRAF tasks, such as bias subtraction, flat-field normalization, and wavelength calibration. We have done flux calibrations, and extinction corrections with the E(B-V) values taken from the literature. Table 2 shows the object designations (Column 1), the E(B-V) values (Column 2), and their respective references (Column 3). Spectrophotometric standards from Hamuy et al. (1994) were observed, too.

In the linearized spectra the line intensities have been measured by the conventional method, adjusting a gaussian function to the profile. Uncertainties in the line intensities come mainly from the position of the underlying continuum. We estimate the errors in the measures to be about 20% for the weakest lines (line fluxes  $\approx 10$  on the scale of  $H\beta = 100$ ) and about 10% for the strongest lines.

In the  $5500\text{\AA}$  region, the S/N ratio in the continuum is approximately 55 for the

Cassegrain spectrum obtained on 1998 March 14 and 50 for the one obtained on 2000 June 9. In the 3600 Å region, the S/N ratio for the Cassegrain spectrum is approximately 35. Since there is no completely line free region in the spectrum, the S/N derived is an upper limit.

In addition to the FEROS and Cassegrain data, we also obtained spectra with medium resolution, using a Coudé spectrograph. These Coudé data came from the 1.6m telescope at the Laboratório Nacional de Astrofísica, Brasópolis (Brazil). We obtained spectra for HD 326823 and six other objects using an instrumental setup with a grating with  $600 \text{ l mm}^{-1}$ , providing a resolution of  $\sim 0.8 \text{ Å}$  in the range 9800-10200 Å. The data reduction has been performed using standard IRAF tasks, too. Table 3 shows the log of the observations.

### 3. The Spectral Atlas

In order to identify the lines, we have used the line lists provided by Moore (1945), Thackeray (1967), and Landaberry, Pereira, & Araújo (2001). We also looked up two sites on the web: NIST Atomic Spectra Database Lines Form (URL [physics.nist.gov/cgi-bin/AtData/lines\\_form](http://physics.nist.gov/cgi-bin/AtData/lines_form)) and The Atomic Line List v2.04 (URL [www.pa.uky.edu/~peter/atomic/](http://www.pa.uky.edu/~peter/atomic/)).

Tables 4 and 5 show the observed wavelength (Column 1), the proposed identification (Column 2), and the measured line equivalent width (W) (Column 3) for emission and absorption lines, respectively, present in the HD 326823 FEROS spectrum. There are 10 lines that remain unidentified and they are labelled as "Uid" in Column 2. Figures 1a, 1b, and 1c present this FEROS spectrum; the strongest lines ( $W > 1 \text{ Å}$ ) are marked.

Table 6 presents the observed wavelength (Column 1), the proposed transitions (Column 2), and intensities in  $\text{ergs cm}^{-2} \text{ s}^{-1}$  ( $I(\lambda)$ ) (Column 3) for emission lines in the

low resolution spectrum in the spectral range 3060-4060 Å. We note that due to the low efficiency of the detector in the violet region, we were able to identify only a few lines between 3600 and 4060 Å.

Tables 7 and 8 concern the emission and absorption lines respectively, present in the low resolution spectra with spectral ranges 3600-7400 Å and 3800-8700 Å. Columns 1 and 2 in the tables show the observed wavelengths and the measured line intensities, respectively, for the spectrum taken on 1998 March 14. Columns 3 and 4 show the same data for the spectrum taken on 2000 June 9. Finally, Column 5 presents the proposed identifications. The intensities shown in these two tables are relative to  $H\beta = 100$  and as  $H\beta$  is in emission, we decided to put the minus signal before the intensity values of absorption lines. We found that many emission lines are more intense than  $H\beta$ , especially He I lines. In general, there is a rather significant difference between line intensities of the two dates. In most cases there was an increase between the spectrum taken on 1998 March 14 and that on 2000 June 9. On the contrary, no significant change is seen in the continuum (Figure 2). With the help of the FEROS spectrum, we have been able to deblend, for instance, the feature observed at 5046.9 Å, estimating the contributions of the N II 5045.1 Å, Si II 5047.3 Å, and He I 5047.7 Å lines. These values are shown in Table 7.

The column labelled “Identification” in the tables has the element transition, the multiplet, and the rest wavelength of the transition. It is important to say that since different sources were consulted, it is possible that more than one ion can be allocated to a single feature. In these cases, we give some possible alternative identifications.

Our spectra confirmed, in the optical region, the predominance of He I, Fe II, and N II lines, and the weakness of H transitions. In the next section we will comment on the most interesting features and measurements obtained with FEROS, Cassegrain, and Coudé data and discuss the nature of HD 326823.

## 4. Discussion

### 4.1. FEROS Spectrum

Thanks to its high resolution, the FEROS spectrum leads to the identification of a great number of lines and to a better definition of their profiles. It also allowed us to obtain individual equivalent widths of features blended in the Cassegrain spectra and so to evaluate the intensity of each line.

He I 3889 Å, 4922 Å, 5016 Å, 5876 Å, 6678 Å, 7065 Å and 7281 Å transitions are among those with the highest equivalent widths. These lines present a two-peak structure with blue and red edges reaching  $200 \text{ km s}^{-1}$  (Figure 3). The He I 3889 Å central absorption is very strong; it suggests the effect of diluted radiation (see e.g. Niemela & Sahade 1980).

Regarding H lines, we are only sure of the identification of H $\alpha$  and H $\beta$ . The presence of P17 is uncertain. H $\alpha$  and H $\beta$  also reveal a two-peak structure (Figure 4). It is important to compare the strength of He and H lines. For instance, He I 4713 Å is stronger than H $\beta$  while He I 6678 Å is comparable to H $\alpha$ . This behavior is confirmed by the low resolution spectra (see Table 7).

N lines are numerous and conspicuous. We have identified several permitted N I emission lines as well as permitted and forbidden N II transitions. It is curious that the majority of the permitted N II lines are in absorption. This seems to indicate a photospheric origin for them. The forbidden lines are all in emission, indicating that they are formed in the star's envelope. In Figure 5 we can see some N II profiles.

We have found many permitted and forbidden emission lines attributed to low ionization metals, specially Fe II. However, these lines are not very strong. Others elements identified are Si II, O II, and Cr II. We also found that two lines of the red Ca II triplet have a high equivalent width and show the two-peak structure, confirming Lopes et al.



(1992). Unfortunately, we cannot measure the third line's (8540 Å) equivalent width due to the existence of a gap in this spectral region. In addition, we identified some interstellar absorption bands (4430 Å, 5780 Å, 5797 Å) and also IS lines due to Ca II (3934 Å and 3968 Å), CH<sup>+</sup> (3958 Å, 4233 Å) and Na I (5890 Å, 5896 Å).

## 4.2. Cassegrain Spectra

The importance of the low resolution spectra is to show the continuum behavior and to allow the measurement of line intensities, thanks to the flux calibration. Below, the spectra in two different wavelength ranges are briefly described. A comparison with other stars observed by us is presented, too.

### 4.2.1. 3060 Å - 4060 Å

This spectrum has a wavelength range of  $\sim 1000$  Å and it shows the behavior of the continuum from the UV to the blue region. We were able to identify only a few lines in this region due to the noise. The most remarkable feature is the He I 3888.7 Å. In Figure 6, we show the spectra of HD 326823, HD 316285, and HD 327083. The HD 326823 spectrum in this figure is the one obtained on 1998 July 12. The HD 316285 spectrum shows many lines of the Balmer series, with P-Cygni profiles. In HD 327823 these lines are in absorption. So, once more we note clearly a H deficiency in HD 326823.

### 4.2.2. 3600 Å - 7400 Å and 3800 Å - 8700 Å

These spectra cover a wavelength range of  $\sim 4000$  Å and they show the behavior of the continuum from the blue to the red region.

Figure 7 presents a comparison between HD 326823 and five other stars: HD 87643, classified as B[e]sg (Miroshnichenko 1998; Oudmaijer 1998 & Oudmaijer et al. 1998) and as Iron Star (Walborn & Fitzpatrick 2000); HD 316285, classified as LBV (Hillier et al. 1998) and as Iron Star (Walborn & Fitzpatrick 2000); HD 327083, classified as LBV or B[e]sg (Machado, de Araújo, & Lorenz-Martins 2001);  $\eta$  Car, classified as LBV (Walborn 1995); and HR Car, classified as LBV, too (Hutsemekers & van Drom 1991). The HD 326823 spectrum in this figure is the one obtained on 1998 March 14.  $H\alpha$ ,  $H\beta$ , and the stronger He I lines are marked. We can see in this figure that only HD 326823 has He I lines more intense than  $H\alpha$  and  $H\beta$ . These data contribute to the assertion that HD 326823 is in an advanced evolutionary stage.

### 4.3. Coudé Spectrum

Figure 8 shows our Coudé spectra of HD 326823 and five other similar objects. HD 326823 is the only one that shows the Fe II 9997 Å transition (with two-peak structure) much more intense than  $P\delta$ . Moreover, the He I 10031 Å line is at least as strong as  $P\delta$ , confirming the H deficiency in HD 326823.

### 4.4. The nature of HD 326823

Our data confirm that HD 326823 exhibits remarkably strong He I lines. On the contrary, the few H I transitions seen are unusually weak. The He/H line intensity ratios provide clear evidence for He overabundance. Such a conclusion is reinforced by the comparison made in previous subsections with some objects generally classified as B[e] supergiants (B[e]sg), Luminous Blue Variables (LBV) or “Iron Stars” (Lamers et al. 1998; Walborn & Fitzpatrick 2000). Moreover our spectra reveal a great number of conspicuous

N II transitions. N I emissions and (perhaps) few N III absorption lines may also be seen, but the dominant ion of this species is surely N II. On the other hand, C lines are not seen at all. Concerning oxygen, only the O I 4661.2 Å and the O II 6046 Å transitions seem to be present in emission. The identification of O II 7319 Å to the feature seen at 7321.8 Å is rather doubtful, since the contribution of the Fe II 7320.7 Å (m7) is probably much more important (we note that other Fe II lines of the same multiplet are present). Thus, it is likely that N is overabundant too. These conclusions point in favour of considering HD 326823 as an evolved object.

Let us compare now HD 326823 with other peculiar, evolved massive stars. Due to the absence of the N IV 4058 Å, the N III 4630-4634 Å, and the He II 4686 Å emissions, it can not be considered as a WNL or WN9ha star (Walborn & Fitzpatrick 2000). For the same reason it may not be classified as Ofpe/WN9 (Walborn 1982). As N lines are concerned, the spectra of HD 326823 is more or less similar to those of some WNVL stars (Walborn & Fitzpatrick 2000). However, in such objects the H I recombination lines are the most prominents. Finally, the group of “Iron Stars”, sometimes cited in the literature, is not very useful since the objects generally put in this category have diverse physical natures. We are tempted to conclude that HD 326823 is an unique peculiar star.

In the last years several works have been devoted to massive stars in transition. From optical spectroscopy of Ofpe/WN9 and related stars, Nota et al. (1996) suggested that Of, Ofpe/WN9, LBV, and B[e] stars must be considered within the same evolutionary scenario. On the basis of infrared spectra, Morris et al. (1996) concluded that Of supergiants, Ofpe/WN9, WNL, B[e] supergiants, and LBV, are transitional in their morphological classification and may be related in their evolution. Some years before Schulte-Ladbeck et al. (1993) proposed that the distinction between the B[e] supergiants and other transition objects is a stronger degree of nonspherical symmetry in their envelopes, probably due to

the higher rotational velocities. We note the apparent disk line profiles seen in our data, which suggest that HD 326823 may have been a rapid rotator.

From the theoretical point of view two different scenarios have been proposed to describe the stages between O and WR stars. Crowther et al. (1995) suggested that the WNL phase follows directly from the Of stars, at least for the objects with the highest initial masses. The WNL would then evolve to WNE and finally WC stars. Langer et al. (1994) proposed the following sequence:  $O \rightarrow Of \rightarrow \text{H-rich WN} \rightarrow \text{LBV} \rightarrow \text{H-poor WN} \rightarrow \text{H-free WN} \rightarrow \text{WC} \rightarrow \text{SN}$ . In this picture, HD 326823 could be in a post-LBV stage, close to the H-poor WN phase. Such a statement is hampered by the absence of an abundance analysis, that is beyond the scope of the present paper.

In summary it is certain that HD 326823 is an indeed peculiar object, which is in an evolved evolutionary phase of the massive stars. It might be the only known example of a very precise, short-lived stage. However, its real nature can not be ascribed until we have accurate determinations of some physical parameters as the mass-loss rate and the helium and nitrogen abundances.

The authors thank the useful comments and suggestions of an anonymous referee, which improved the present paper. M.B.F. acknowledges financial support from CAPES-Brazil (PhD studentship).

## REFERENCES

- Carlson, E. D., & Henize, K. G. 1979, *Vistas in Astronomy*, 23, 213
- Crowther, P. A., Smith, L. J., Hillier, D. J., & Schmutz, W. 1995, *A&A*, 293, 427
- de Winter, D., & Pérez, M. R. 1998, *B[e] Stars* (Dordrecht: Kluwer Academic Publishers)
- Feast, M. W., Stoy, R. H., Thackeray, A. D., & Wesselink, A. J. 1961, *MNRAS*, 122, 239
- Feinstein, A., Marraco, H. G., & Muzzio, J. C. 1973, *A&AS*, 12, 331
- Hamuy, M., Suntzeff, N. B., Heathcote, S. R., Walker, A. R., Gigoux, P., & Phillips, M. M. 1994, *PASP*, 106, 566
- Hillier, D. J., Crowther, P. A., Najarro, F., & Fullerton, A. W. 1998, *A&A*, 340, 483
- Hutsemekers, D., & van Drom, E. 1991, *A&A*, 248, 141
- Kaufer, A., Stahl, S., Tubbesing, S., Norregard, P., Avila, G., Francois, P., Pasquini, L., & Pizzella 1999, *The Messenger*, 95, 8
- Kozok, J. R. 1985, *A&AS*, 62, 7
- Lamers, H. J. G. L. M., Zickgraf, F.-J., de Winter, D., Houziaux, L., & Zorec, J. 1998, *A&A*, 340, 117
- Landaberry, S. J. C., Pereira, C. B., & de Araújo, F. X. 2001, *A&A*, submitted
- Langer, N., Hamann, W. -R., Lennon, M., Najarro, F., Pauldrach, A. W. A., & Puls, J. 1994, *A&A*, 290, 819
- Lopes, D. F., Damineli, A., & de Freitas Pacheco, J. A. 1992, *A&A*, 261, 482
- Machado, M. A. D., de Araújo, F. X., & Lorenz-Martins, S. 2001, *A&A*, 368, L29

- McGregor, P. J., Hyland, A. R., & Hillier, D. J. 1988, *ApJ*, 324, 1071
- Miroshnichenko, A. S. 1998, *B[e] Stars* (Dordrecht: Kluwer Academic Publishers)
- Moore, C. E. 1945, *A Multiplet Table of Astrophysical Interest, Part I - Table of Multiplets*  
(Revised Ed., Princeton, New Jersey: Princeton University Observatory)
- Morris, P. W., Eenens, P. R. J., & Blum, R. D. 1996, *ApJ*, 470, 597
- Niemela, V. S., & Sahade, J. 1980, *ApJ*, 238, 244
- Nota, A., Pasquali, A., Drissen, L., Leitherer, L., Robert, C., Moffat, A. F. J., & Schmutz, W. 1996, *ApJS*, 102, 383
- Oudmaijer, R. D. 1998, *B[e] Stars* (Dordrecht: Kluwer Academic Publishers)
- Oudmaijer, R. D., Proga, D., Drew, J. E., & de Winter, D. 1998, *MNRAS*, 300, 170
- Schulte-Ladbeck, R. E., Leitherer, C., Clayton, G. C., Robert, C., Meade, M. R., Drissen, L., Nota, A., & Schmutz, W. 1993, *ApJ*, 407, 723
- Sheikina, T. A., Miroshnichenko, A. S., & Corporon, P. 2000, *The Be Phenomenon in Early-Type Stars*, IAU Colloquium, 175, in press
- Shore, S. N., Brown, D. N., Bopp, B. W., Robinson, C. R., Sanduleak, N., & Feldman, P. D. 1990, *ApJS*, 73, 461
- Stephenson, C. B. 1974, *ApJ*, 191, 685
- Sterken, C., Stahl, O., Wolf, B., Th. Szeifert, & Jones, A. 1995, *A&A*, 303, 766
- Thackeray, A. D. 1967, *MNRAS*, 135, 51
- van Genderen, A. M., et al. 1990, *A&AS*, 82, 189

Walborn, N. R. 1982, *ApJ*, 256, 45

Walborn, N. R. 1995, *RevMexAA*, 2, 51

Walborn, N. R., & Fitzpatrick, E. L. 2000, *PASP*, 112, 50

Zorec, J. 1998, *B[e] Stars* (Dordrecht: Kluwer Academic Publishers)

Fig. 1.— The spectral atlas from 3800 to 5600 Å obtained from the FEROS spectrum. The strongest lines ( $W > 1$  Å) are marked.

Fig. 2.— The spectral atlas from 5600 to 7400 Å obtained from the FEROS spectrum. The strongest lines ( $W > 1$  Å) are marked.

Fig. 3.— The spectral atlas from 7400 to 9200 Å obtained from the FEROS spectrum. The strongest lines ( $W > 1$  Å) are marked.

Fig. 4.— The HD 326823 low resolution spectra, obtained on 1998 March 14 and on 2000 June 9. These spectra were corrected for extinction, using  $E(B-V)$  values.

Fig. 5.— Profiles of six He I lines presented in the FEROS spectrum.

Fig. 6.—  $H\alpha$  and  $H\beta$  profiles shown in the FEROS spectrum.

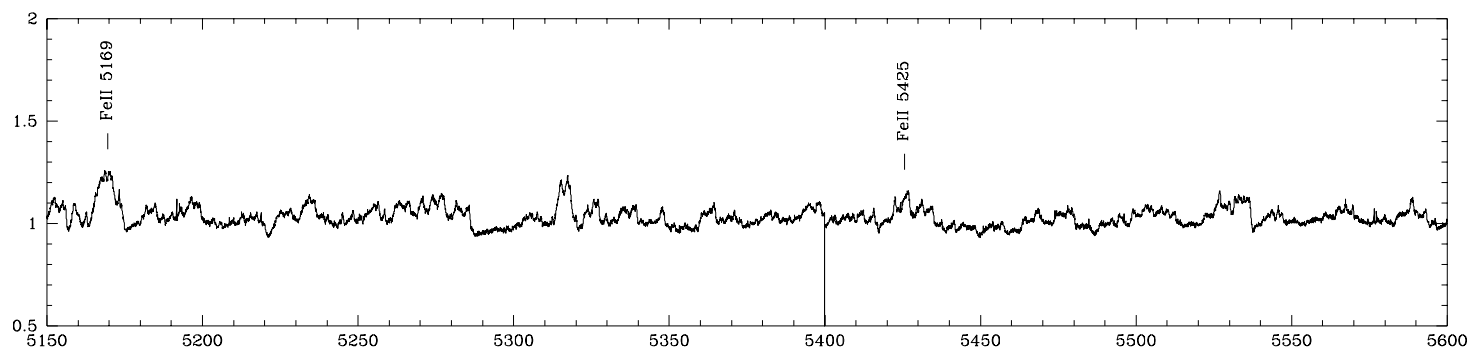
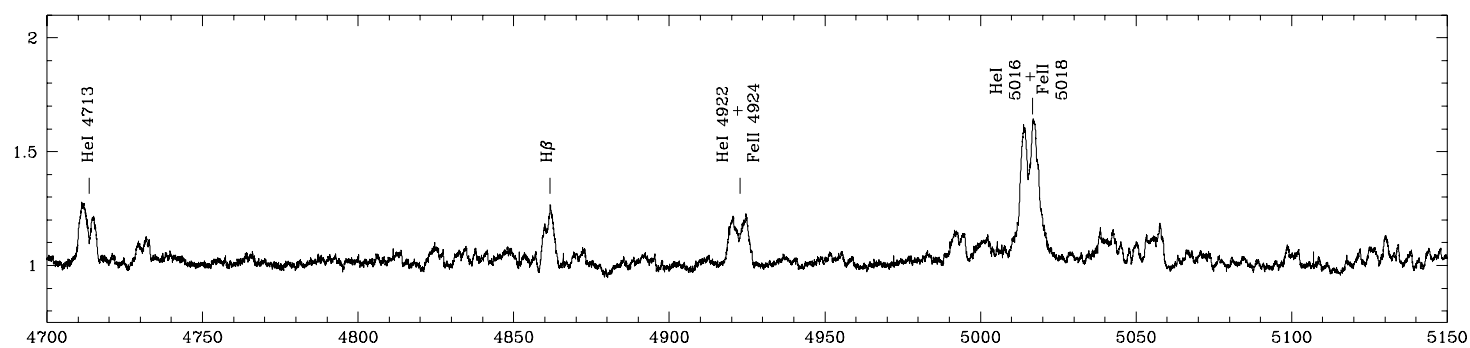
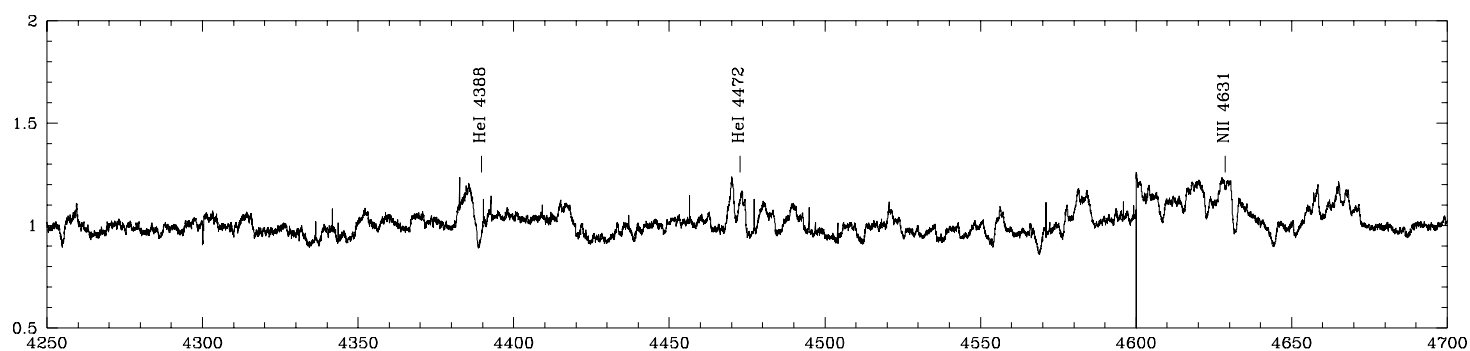
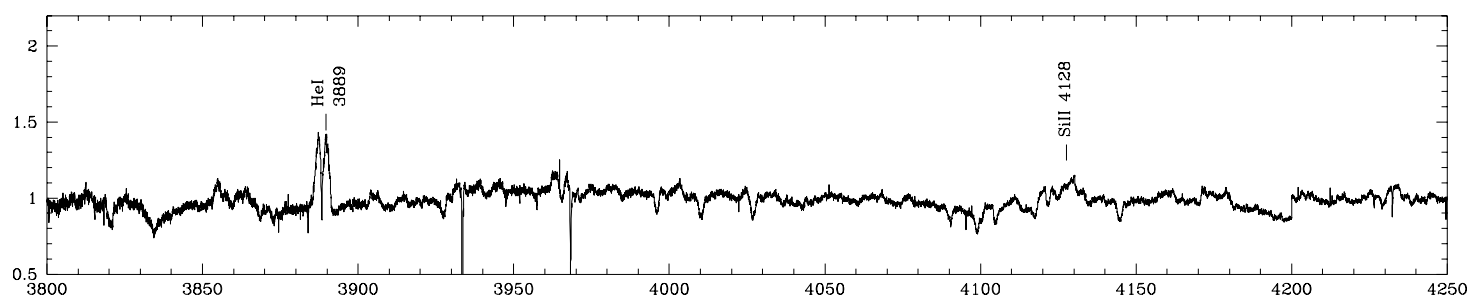
Fig. 7.— Profiles of permitted and forbidden N II lines obtained from FEROS spectrum.

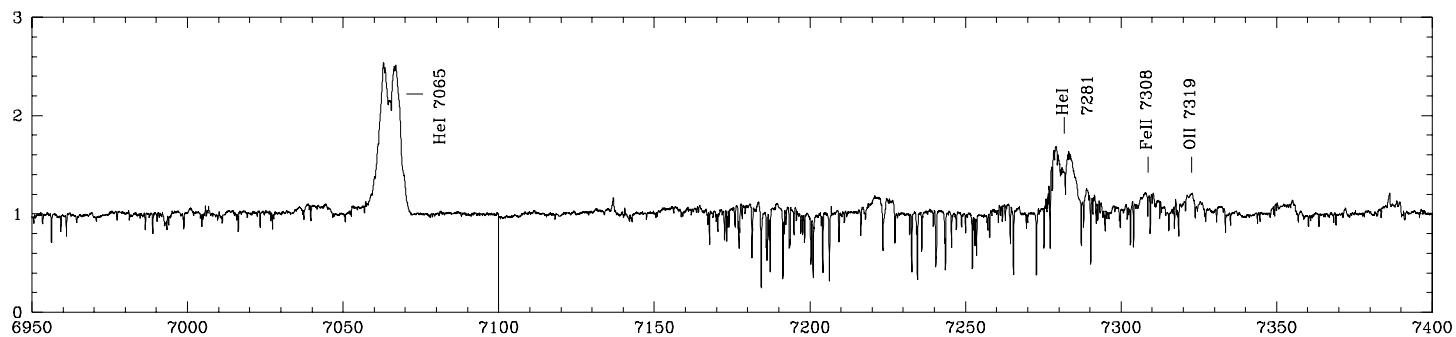
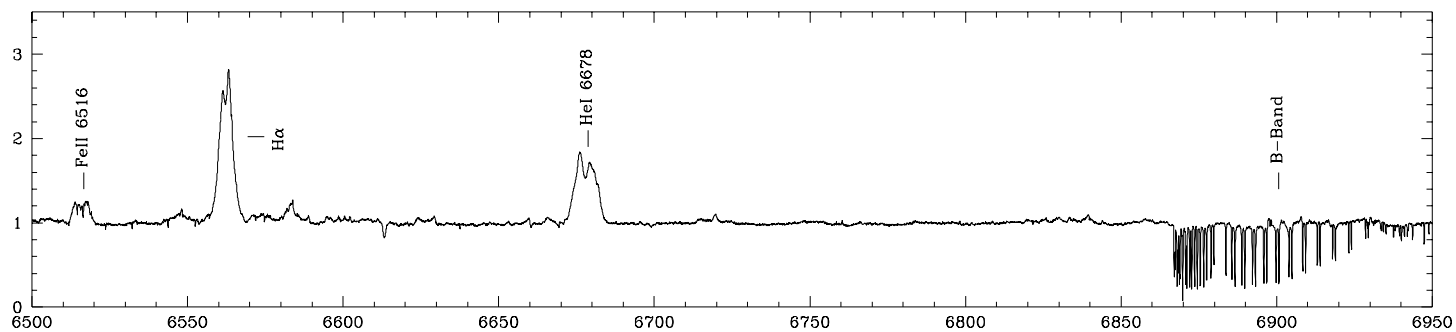
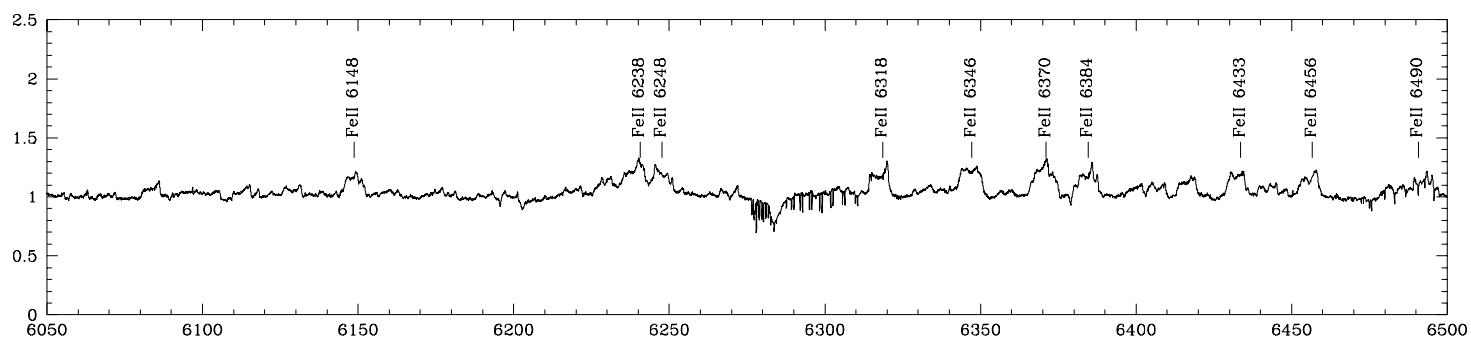
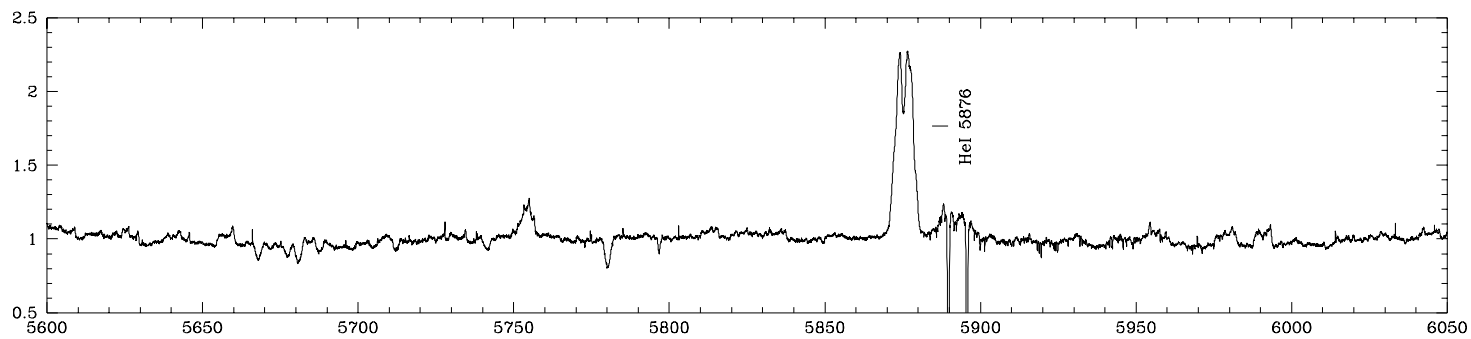
Fig. 8.— Low resolution spectra of HD 326823, HD 316285, and HD 327083 with  $\lambda_{central} \sim 3600\text{\AA}$ .

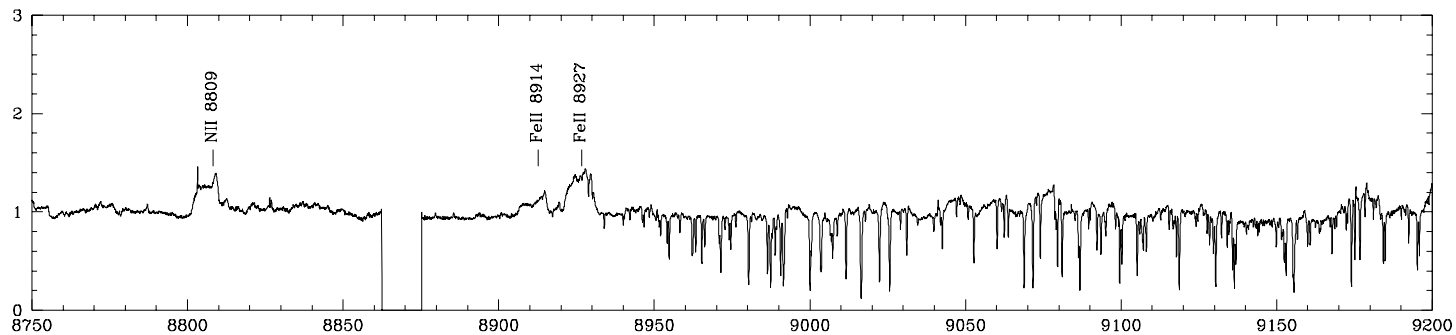
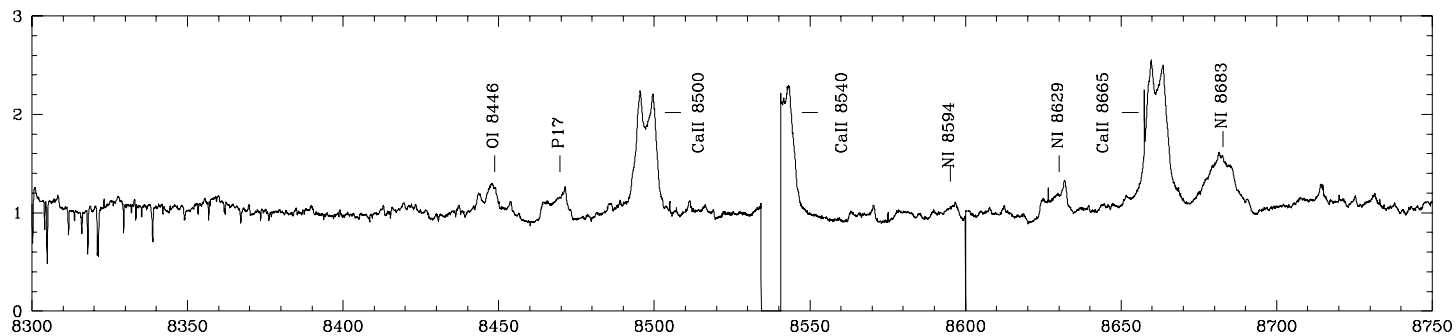
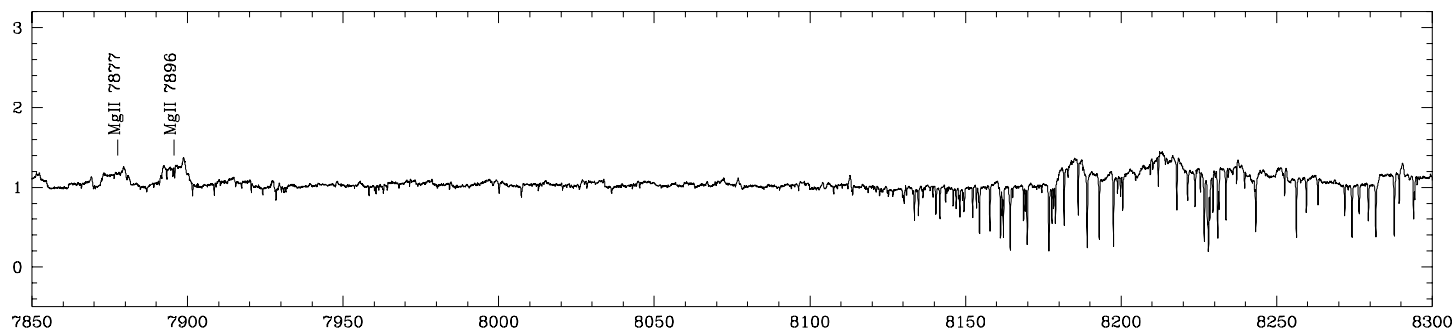
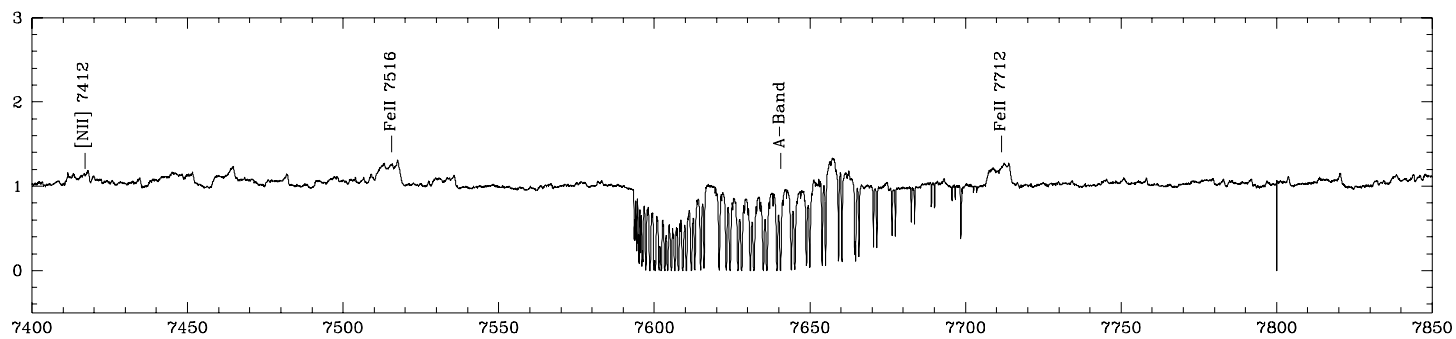
Fig. 9.— Normalized low resolution spectra of HD 326823, HD 87643, HD 316285, HD 327083, HR Car, and  $\eta$  Car.

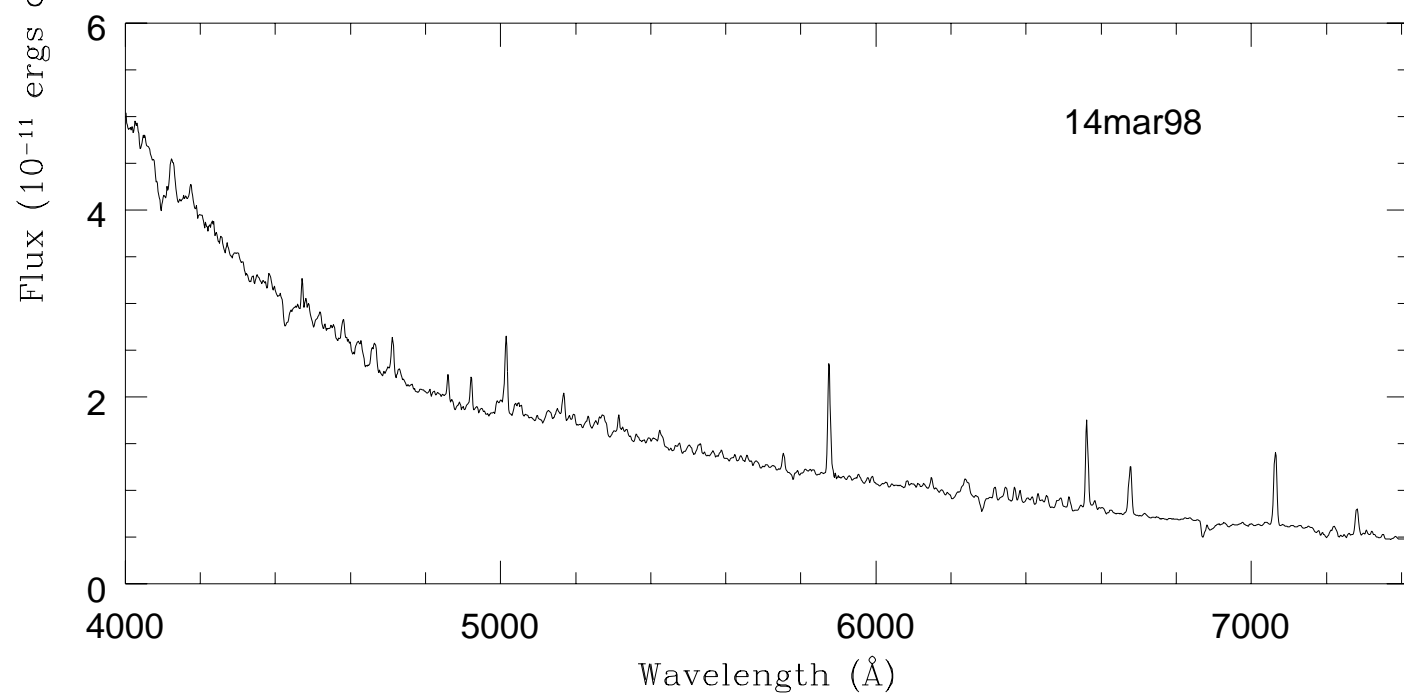
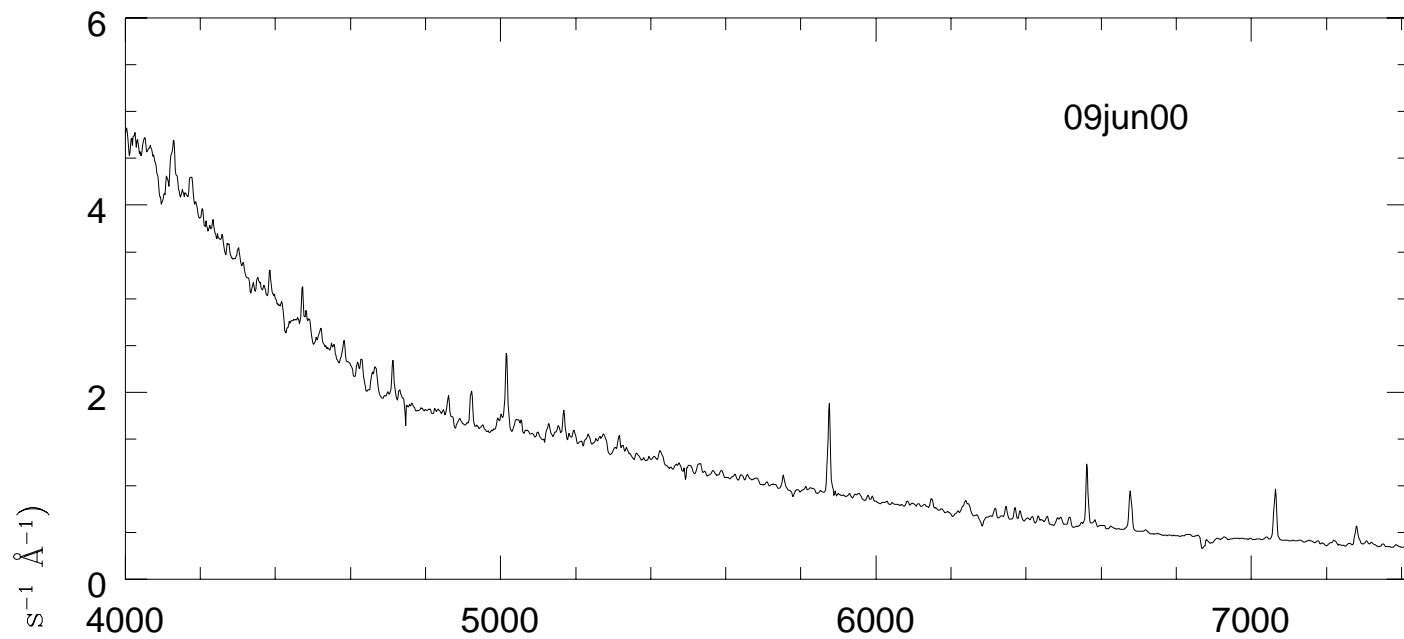
Fig. 10.— Normalized Coudé spectra of HD 326823, HD 87643, HD 316285, HD 327083, CPD-52°9243, HR Car, and GG Car.

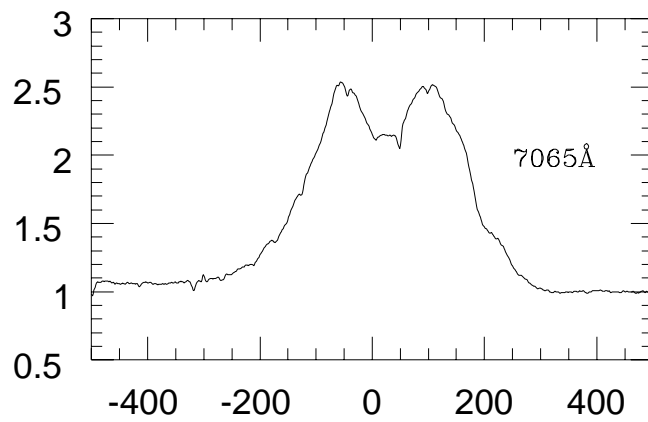
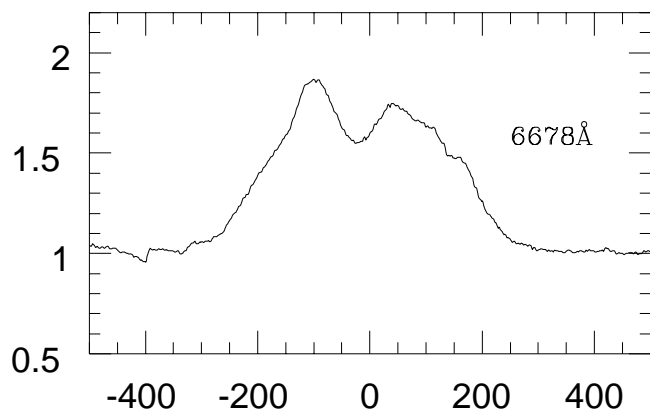
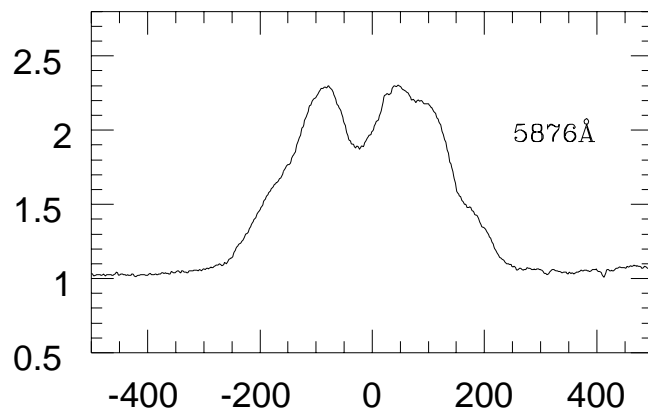
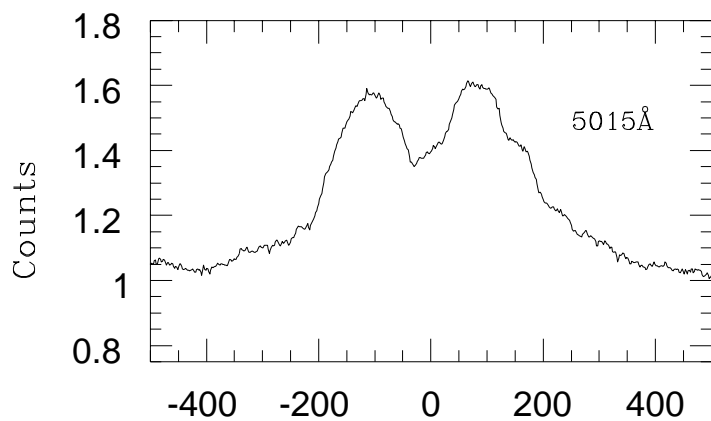
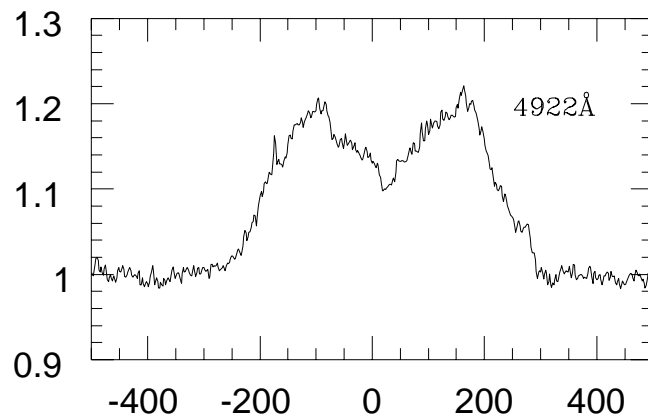
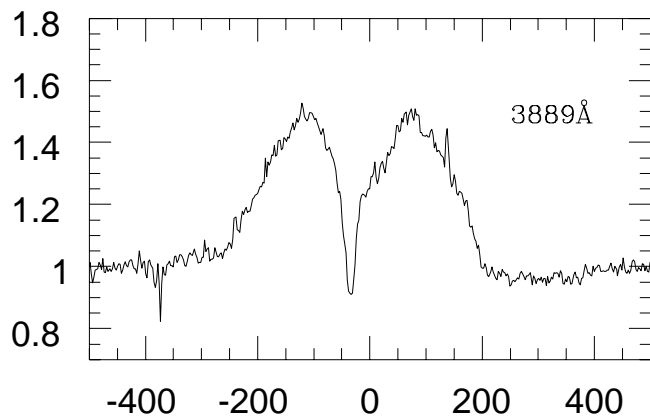




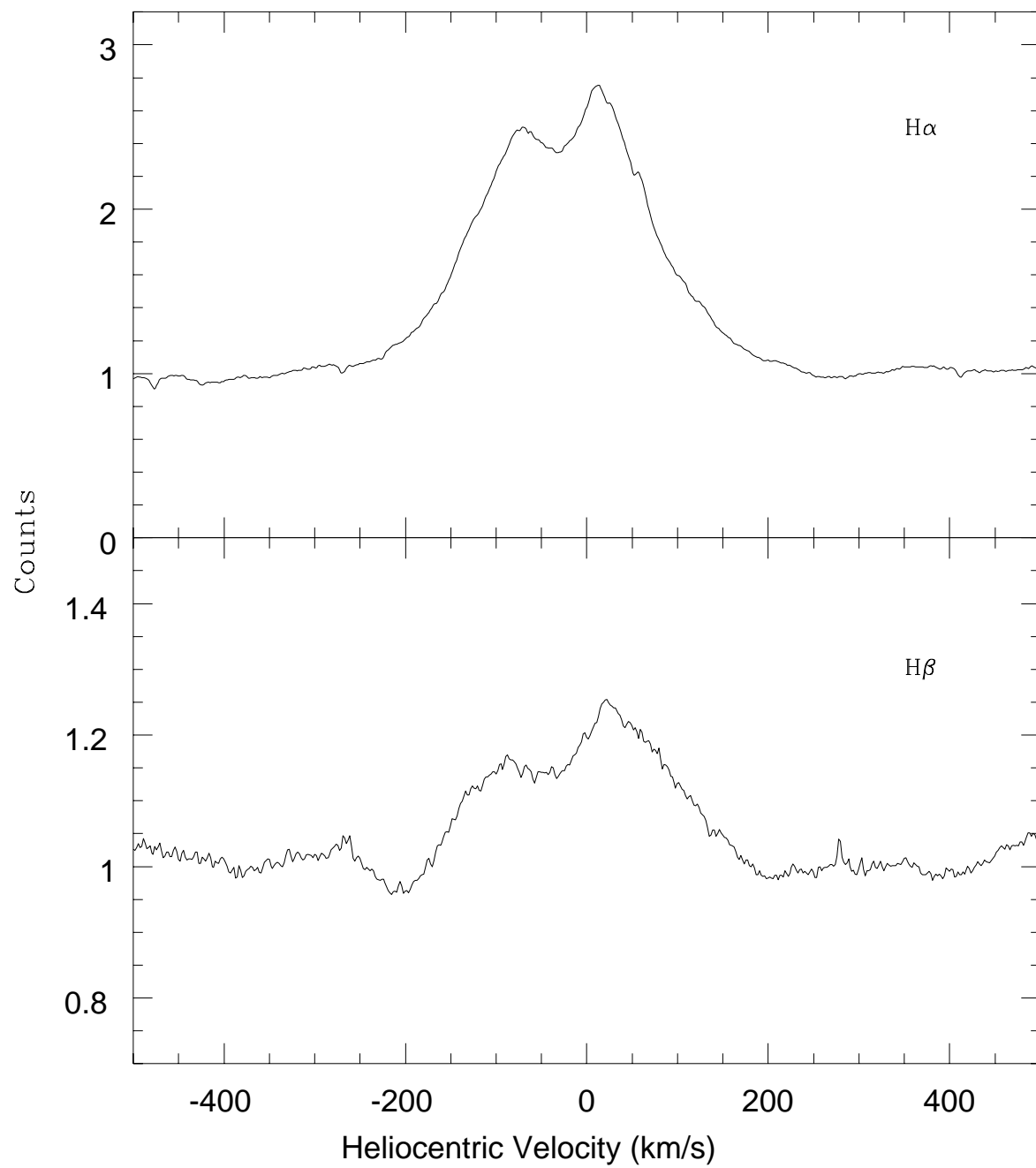


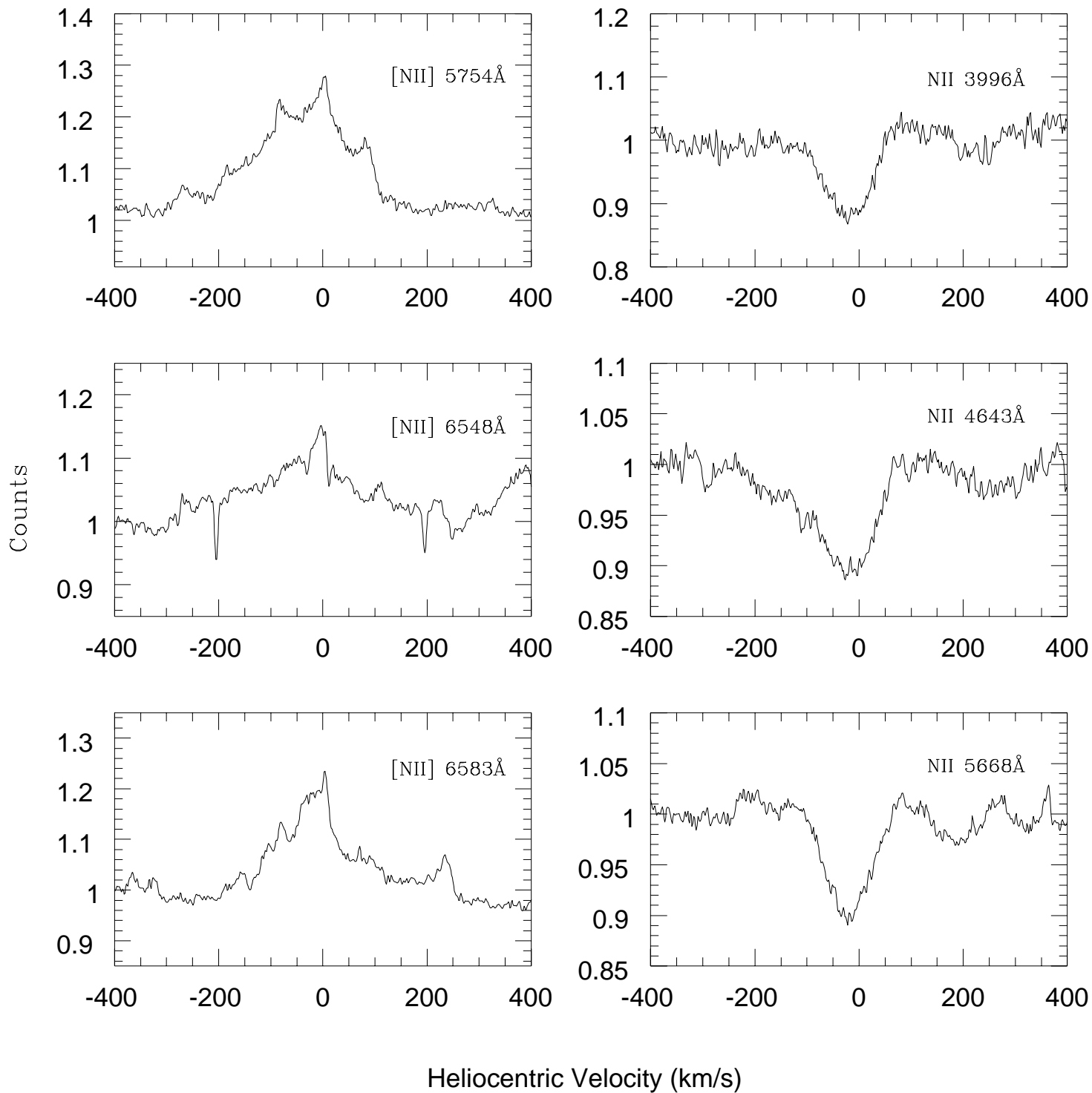


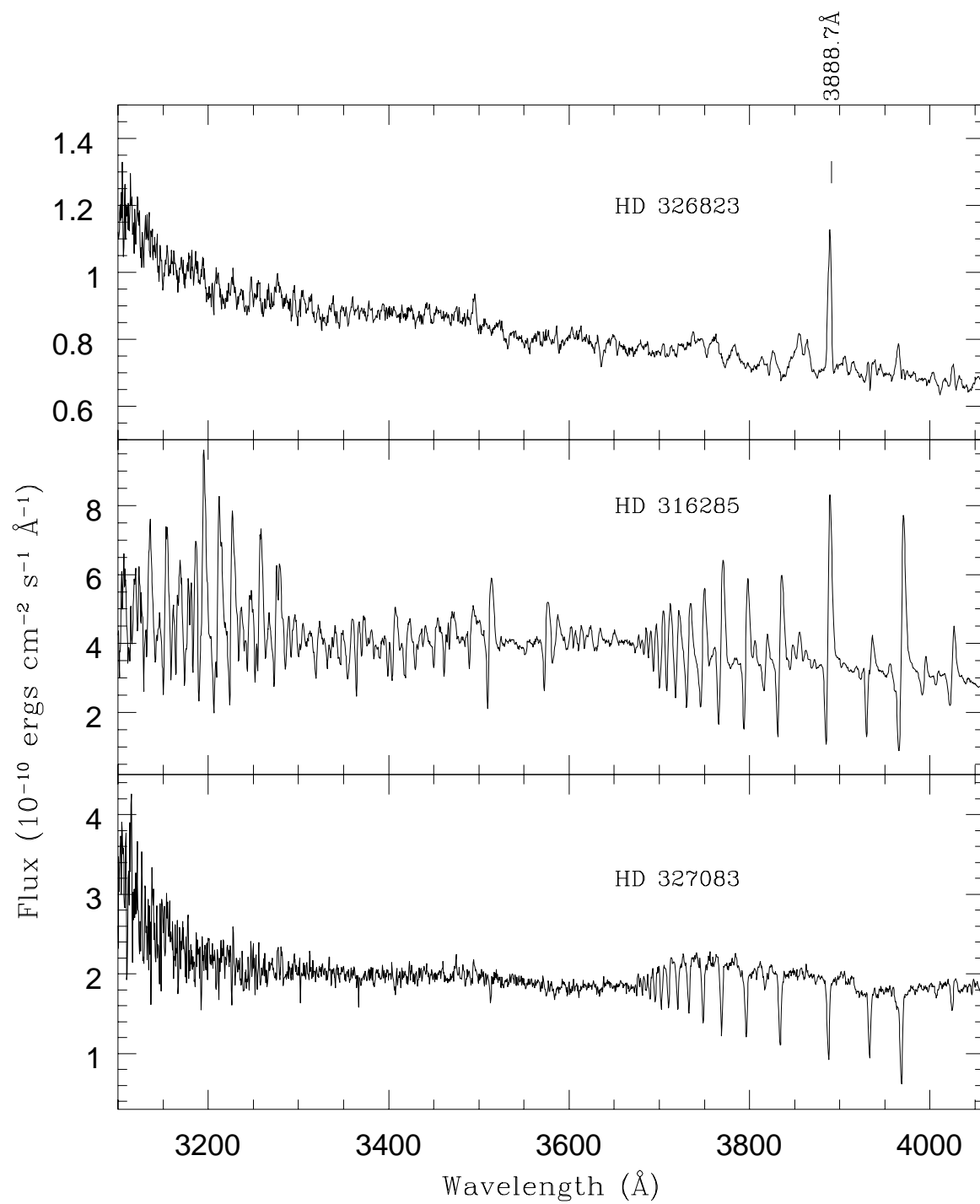




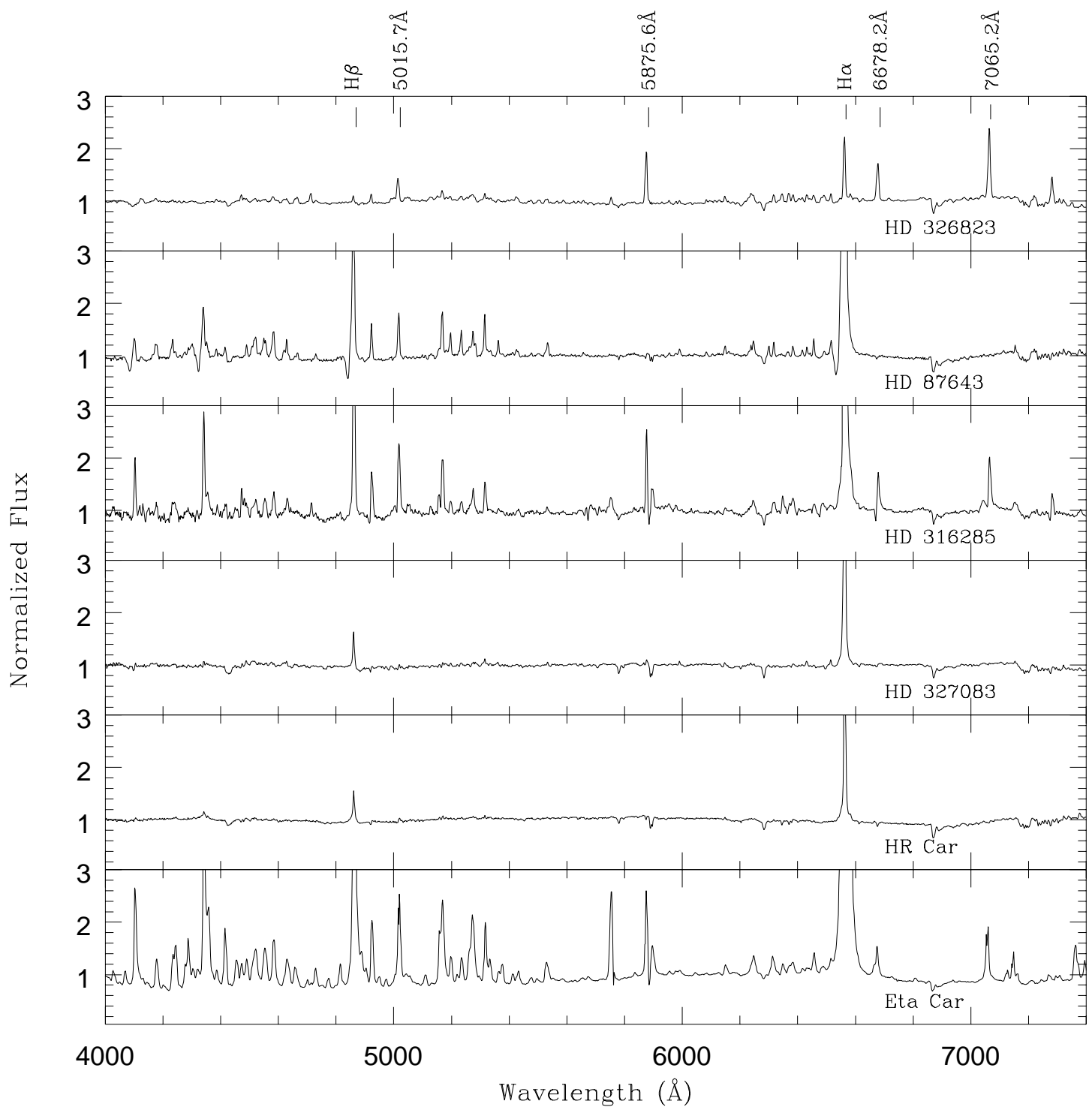
Heliocentric Velocity (km/s)











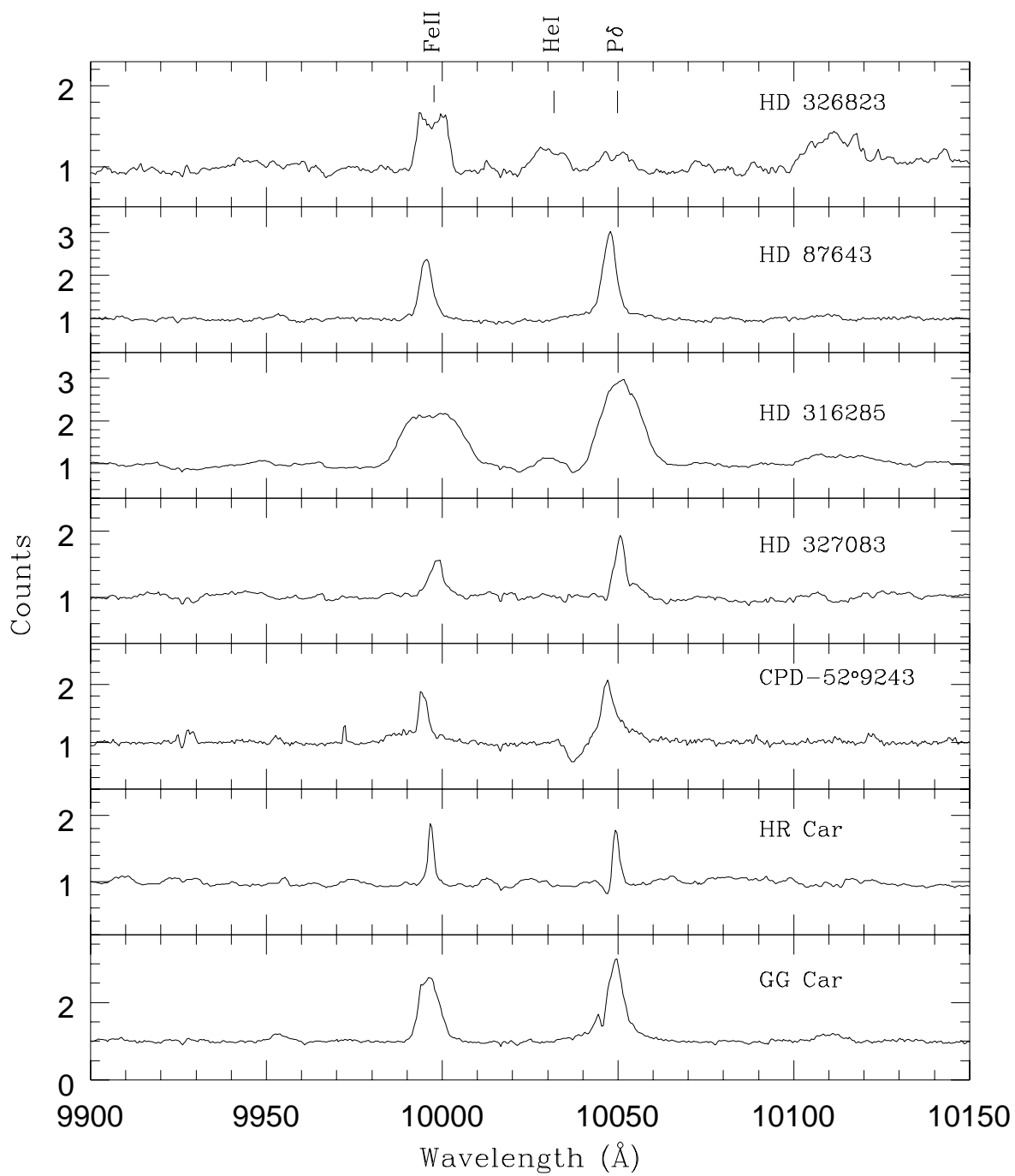


TABLE 1  
OBSERVATION LOG OF CASSEGRAIN DATA.

Object	Date	Wavelength Range	Exp Time (sec)
HD 326823	1998 Mar 14	3600 Å - 7400 Å	60
HD 326823	1998 Jul 12	3060 Å - 4060 Å	300
HD 326823	2000 Jun 9	3800 Å - 8700 Å	30
HR Car	1998 Mar 11	3600 Å - 7400 Å	25
HD 87643	1998 Mar 11	3600 Å - 7400 Å	20
HD 316285	1998 Jul 11	3060 Å - 4060 Å	600
HD 316285	1998 Mar 14	3600 Å - 7400 Å	5
HD 327083	1998 Jul 12	3060 Å - 4060 Å	300
HD 327083	1998 Mar 14	3600 Å - 7400 Å	50
$\eta$ Car	1999 Dec 18	3600 Å - 7800 Å	15

TABLE 2  
E(B-V) USED FOR EXTINCTION CORRECTION.

Object	E(B-V)	Reference
HD 326823	1.12	1
HD 87643	0.32	2
HR Car	0.90	3
$\eta$ Car	1.20	4
HD 316285	1.81	5
HD 327083	1.80	6

REFERENCES.—(1) Kozok 1985; (2) Zorec 1998; (3) van Genderen et al. 1990; (4) Feinstein, Marraco, & Muzzio 1973; (5) Hillier et al 1998; (6) Sheikina et al. 2000.

TABLE 3  
OBSERVATION LOG OF COUDÉ DATA.

Object	Date	Wavelength Range	Exp Time (sec)
HD 326823	1998 Sept 13	9800 Å - 10200 Å	1800
HR Car	1999 Apr 25	9800 Å - 10200 Å	900
GG Car	1998 Apr 13	9800 Å - 10200 Å	1200
HD 87643	1998 Apr 13	9800 Å - 10200 Å	1200
HD 316285	1998 Sept 12	9800 Å - 10200 Å	1500
HD 327083	1998 Sept 11	9800 Å - 10200 Å	1800
CPD-52°9243	1998 Apr 14	9800 Å - 10200 Å	1800

TABLE 4

OBSERVED EMISSION LINES AND THEIR EQUIVALENT WIDTHS, OBTAINED WITH THE FEROS SPECTROGRAPH.

Wavelength ( $\text{\AA}$ )	Identification	W ( $\text{\AA}$ )
3888.3	He I (m2) 3888.7	2.90
4126.9	Si II (m3) 4128.1	1.70
	Si II (m3) 4130.9	
4175.4	Fe II (m27) 4173.5	0.84
4233.0	Fe II (m27) 4233.2	0.44
4302.2	Fe II (m27) 4304.4	0.34
4359.8	Fe II [m6F] 4358.1	0.23
	Fe II [m21F] 4358.4	
	Fe II [m7F] 4359.3	
4369.1	Fe II [m21F] 4372.4	0.26
4374.4	N II (m16) 4375.0	0.36
4461.1	Uid	0.31
4471.4	He I (m14) 4471.5	1.11
4480.8	Mg II (m4) 4481.3	0.76
4490.1	Fe II [m6F] 4488.8	0.69
	Fe II (m37) 4491.4	
4507.7	Fe II (m38) 4508.3	0.46
	Fe II [m6F] 4509.6	
4519.5	Fe II (m37) 4520.2	0.98
	Fe II (m38) 4522.6	
4548.9	Fe II (m38) 4549.5	0.43
4582.8	Fe II (m37) 4582.8	0.72
	Fe II (m38) 4583.8	
	Fe II (m26) 4584.0	
4627.9	Fe II (m37) 4629.4	1.22
	N II (m5) 4630.5	
4657.8	N II (m11) 4654.5	0.23
	Fe II (m43) 4657.0	
	Fe II [m3F] 4658.1	
4662.2	O II (m1) 4661.2	0.17
4665.1	Fe II (m44) 4663.7	0.40
	Fe II [m4F] 4664.5	
	Fe II (m17) 4664.8	
	Fe II [m5F] 4665.0	
4669.3	Fe II (m37) 4666.8	0.35
	Fe II [m4F] 4667.0	
	N II (m11) 4667.2	
4712.8	He I (m12) 4713.4	1.38
4730.6	Fe II (m43) 4731.4	0.19
4861.4	H $\beta$ 4861.3	1.06
4871.1	Fe II [m20F] 4874.5	0.26
4922.5	He I (m48) 4921.9	1.39
	Fe II (m42) 4923.9	
4992.7	N II (m24) 4991.2	0.61
	Fe II (m36) 4993.4	

TABLE 4

OBSERVED EMISSION LINES AND THEIR EQUIVALENT WIDTHS, OBTAINED WITH THE FEROS SPECTROGRAPH.

Wavelength ( $\text{\AA}$ )	Identification	W( $\text{\AA}$ )
5001.2	N II (m19) 5001.5	0.44
	Fe II [m20F] 5005.5	
5016.0	He I (m4) 5015.7	3.68
	N II (m19) 5016.4	
	Fe II (m42) 5018.4	
5040.8	Si II (m5) 5041.1	0.59
5044.9	N II (m4) 5045.1	0.14
5047.8	Si II (m15) 5047.3	0.06
	He I (m47) 5047.7	
5050.1	Uid	0.19
5056.1	Si II (m5) 5055.0	0.79
5130.2	Fe III (m5) 5128.8	0.28
5169.3	Fe II (m42) 5169.0	2.09
5183.3	Fe II [m18F] 5182.0	0.36
	Mg I (m2) 5183.6	
	Fe II [m19F] 5184.8	
5193.2	Uid	0.12
5196.5	Fe II (m49) 5197.6	0.40
5234.5	Fe II (m49) 5234.6	0.35
5316.1	Fe II (m49) 5316.6	0.62
	Fe II (m48) 5318.8	
5362.6	Fe II (m48) 5362.9	0.41
5411.6	He II (m2) 5411.5	0.11
5427.4	Fe II (m49) 5425.3	1.22
5433.6	Fe II (m55) 5433.1	0.23
	Fe II [m18F] 5433.2	
5476.9	Fe II [m34F] 5477.3	0.69
	Fe II (m49) 5477.7	
	Cr II (m50) 5479.0	
5505.8	Cr II (m50) 5502.8	0.97
	Cr II (m50) 5503.6	
	Cr II (m50) 5510.1	
5526.8	Fe II [m17F] 5527.3	0.30
	Fe II (m55) 5527.6	
	Fe II [m16F] 5527.6	
5567.0	Uid	0.53
5588.9	Fe II [m39F] 5588.2	0.79
5625.3	Fe II (a2P-b2D) 5627.3	0.12
5642.1	Si II (m14) 5639.5	0.17
	Fe II [m18F] 5644.0	
5658.5	Fe II (m57) 5657.8	0.40
	Fe II [m33F] 5659.8	
5684.5	N II (m3) 5676.0	0.28
	N II (m3) 5679.6	
	N II (m3) 5686.2	
5709.1	N II (m3) 5710.8	0.11
5754.3	N II [m3F] 5754.8	0.84

TABLE 4

OBSERVED EMISSION LINES AND THEIR EQUIVALENT WIDTHS, OBTAINED WITH THE FEROS SPECTROGRAPH.

Wavelength ( $\text{\AA}$ )	Identification	W( $\text{\AA}$ )
5875.6	He I (m11) 5875.6	7.29
5955.4	N II (m28) 5952.4	0.83
5979.3	S III (m4) 5979.0	0.59
5990.9	Fe II (m46) 5991.4	0.61
6048.7	O II (m22) 6046.3	0.11
	O II (m22) 6046.5	
6071.6	He II (m8) 6074.1	0.06
6084.0	Fe II (m46) 6084.1	0.49
6113.5	Fe II (m46) 6113.3	0.37
6129.0	Fe II (m46) 6129.7	0.40
6148.6	Fe II (m74) 6147.7	1.08
6160.4	Fe II (m161) 6160.8	0.30
6239.5	Fe II (m74) 6238.2	2.00
6247.1	Fe II (m74) 6247.6	1.30
6317.7	Fe II (z4D0-c4D) 6318.0	1.30
	Mg I (m23) 6318.2	
6346.6	Fe II (m74) 6345.5	1.73
	Si II (m2) 6347.1	
	Ni II (m46) 6347.1	
6370.5	Fe II (m40) 6369.5	1.84
	Si II (m2) 6371.4	
6384.4	Fe II 6383.8	1.42
6406.6	Ne II (m1) 6407.9	0.58
6416.8	Fe II (m74) 6417.9	0.87
6432.3	Fe II (m40) 6432.7	1.04
6455.9	Fe II (m74) 6456.4	1.17
6489.3	Fe II 6489.6	2.99
6515.9	Fe II (m40) 6516.1	1.65
	Fe II (m72) 6518.2	
6548.1	N II [m1F] 6548.1	0.19
6562.4	He II (m2) 6560.1	8.35
	H $\alpha$ 6562.8	
6588.8	N II [m1F] 6583.6	0.06
6666.1	N II [m2F] 6666.8	0.22
6677.9	He I (m46) 6678.2	5.49
6717.9	S II [m2F] 6716.4	0.34
7040.8	Al II (m3) 7042.1	0.95
7064.9	He I (m10) 7065.2	10.43
7136.7	Ar III 7137.8	0.11
7225.5	Fe II 7224.5	0.50
7261.3	N II (m52) 7259.3	0.98
7281.6	He I (m45) 7281.4	7.11
7308.8	Fe II (m73) 7308.0	1.98
7321.8	O II 7319.0	1.31
	Fe II (m73) 7320.7	
7416.5	N II [m2F] 7411.6	1.04
7446.9	N I (m3) 7442.3	0.64



TABLE 4  
OBSERVED EMISSION LINES AND THEIR EQUIVALENT WIDTHS, OBTAINED WITH THE FEROS SPECTROGRAPH.

Wavelength ( $\text{\AA}$ )	Identification	W( $\text{\AA}$ )
7514.7	Fe II (m73) 7515.9	1.65
7711.2	Fe II [m30F] 7710.8	1.72
7877.3	Mg II (m8) 7877.1	1.59
7895.1	Mg II (m8) 7896.4	1.87
8447.8	O I (m4) 8446.4	1.66
	Fe II [m29F] 8446.1	
8468.7	P17 8469.6	2.36
8497.2	Ca II 8500.4	8.68
8594.4	N I (m8) 8594.1	1.21
8629.5	N I (m8) 8629.2	2.12
8661.4	Ca II 8664.5	10.52
8681.9	N I (m1) 8683.4	5.84
8720.1	N I (m1) 8718.8	0.03
8807.5	N II 8808.6	3.55
8912.0	Fe II 8914.4	2.07
8926.3	Fe II (e4D-5p4D) 8926.7	3.30

TABLE 5

OBSERVED ABSORPTION LINES AND THEIR EQUIVALENT WIDTHS, OBTAINED WITH THE FEROS SPECTROGRAPH.

Wavelength ( $\text{\AA}$ )	Identification	W ( $\text{\AA}$ )
3996.0	N II (m12) 3995.0	0.23
4010.4	He I (m55) 4009.3	0.41
4026.9	He I (m18) 4027.3	0.38
4090.3	Si IV (m1) 4088.9	0.16
4099.0	N III (m1) 4097.3	0.23
	H $\delta$ 4101.7	
4105.2	N III (m1) 4103.4	0.08
	N II (m44) 4110.0	
4115.8	Si IV (m1) 4116.1	0.67
4144.8	He I (m53) 4144.9	0.25
4229.4	N II (m33) 4227.8	0.12
4255.0	Uid	0.15
4286.5	Uid	0.07
4335.3	N III (m10) 4335.5	0.39
4345.7	N III (m10) 4348.4	0.41
4388.9	He I (m51) 4387.9	0.25
	Fe II (m27) 4389.9	
4553.2	Si III (m2) 4552.7	0.37
4568.8	Si III (m2) 4567.9	0.24
4576.1	Si III (m2) 4574.8	0.09
4602.7	N II (m5) 4602.0	0.10
4608.3	N II (m5) 4608.7	0.17
4615.1	N II (m5) 4615.2	0.07
4622.8	Fe II (m38) 4620.5	0.12
	N II (m5) 4622.7	
4631.8	Fe II (m37) 4629.3	0.27
	N II (m5) 4631.8	
4643.9	N II (m5) 4644.4	0.26
4748.8	Uid	0.30
4880.0	N III (m9) 4881.8	0.14
5221.5	Uid	0.24
5667.9	N II (m3) 5668.2	0.24
5671.9	Fe II 5673.2	0.08
5677.4	N II (m3) 5677.6	0.15
5680.8	N II (m3) 5681.1	0.31
5704.9	N III [m14F] 5703.6	0.08
5712.1	N II (m3) 5712.4	0.18
5741.4	Si III (m4) 5739.8	0.19
6202.9	Uid	0.08
6613.2	N II (m31) 6612.4	0.21
7049.1	Uid	0.57

TABLE 6

OBSERVED EMISSION LINE INTENSITIES IN  $\text{ERGS CM}^{-2} \text{ s}^{-1}$ , OBTAINED WITH CASSEGRAIN DATA IN THE 3060 - 4060 Å REGION.

Wavelength (Å)	Identification	I(λ)
3854.2	Si II (m1) 3853.7	$8.15 \times 10^{-13}$
3888.8	He I (m2) 3888.7	$1.94 \times 10^{-10}$
3964.7	He I (m5) 3965.9	$5.66 \times 10^{-11}$
4003.2	Fe II (m190) 4002.6	$1.59 \times 10^{-11}$
	Fe III (m15) 4003.4	
4025.3	He I (m18) 4026.1	$2.92 \times 10^{-11}$
4032.9	Fe II (m126) 4033.0	$1.85 \times 10^{-11}$

TABLE 7  
OBSERVED EMISSION LINE INTENSITIES RELATIVE TO  $H\beta = 100$ , OBTAINED WITH CASSEGRAIN DATA.

Wavelength ( $\text{\AA}$ ) <sup>1</sup>	I( $\lambda$ ) <sup>1</sup>	Wavelength ( $\text{\AA}$ ) <sup>2</sup>	I( $\lambda$ ) <sup>2</sup>	Identification
4125.5	287.5	4128.2	482.4	Si II (m3) 4128.1
				Si II (m3) 4130.9
4174.7	158.3	4175.7	200.0	Fe II (m27) 4173.5
4231.3	62.5	4234.6	38.2	Fe II (m27) 4233.2
4256.7	45.8	—	—	Uid
4301.4	166.7	4301.7	64.7	Fe II (m27) 4304.4
4352.9	14.6	4353.5	22.4	Fe II (m27) 4351.8
				Fe II [m21F] 4352.8
4386.1	79.2	4385.9	100.0	He I (m51) 4387.9
				Fe II (m27) 4389.9
4471.6	91.7	4472.1	129.4	He I (m14) 4471.5
4480.7	33.3	4481.2	35.3	Mg II (m4) 4481.3
4516.5	105.8	4520.4	100.0	Fe II (m37) 4520.2
				Fe II (m38) 4522.6
4552.3	34.2	4552.2	100.0	Fe II (m38) 4549.5
				Si III (m2) 4552.7
4580.9	129.2	4582.6	188.2	Fe II (m37) 4582.8
				Fe II (m38) 4583.8
				Fe II (m26) 4584.0
4623.6	183.3	4624.7	205.9	Fe II (m37) 4629.4
				N II (m5) 4630.5
4662.2	250.0	4664.2	317.7	O II (m1) 4661.2
4710.4	208.3	4713.1	217.7	He I (m12) 4713.4
4731.8	116.7	4733.6	64.7	Fe II (m43) 4731.4
4859.4	100.0	4860.7	100.0	H $\beta$ 4861.3
4922.4	129.2	4922.4	182.4	He I (m48) 4921.9
				Fe II (m42) 4923.9
4993.3	49.6	4993.3	64.7	N II (m24) 4991.2
5001.8	75.0	5001.8	176.5	N II (m19) 5001.5
				Fe II [m20F] 5005.5
5015.7	326.3	5015.7	523.5	He I (m4) 5015.7
				N II (m19) 5016.4
				Fe II (m42) 5018.4
5046.9	116.7	5046.9	152.4	N II (m4) 5045.1
5046.9	50.0	5046.9	65.3	Si II (m15) 5047.3
				He I (m47) 5047.7
5128.5	125.0	5128.5	111.8	Fe III (m5) 5128.8
5168.5	154.2	5168.5	158.8	Fe II (m42) 5169.0
5181.2	83.3	5183.9	47.1	Fe II [m18F] 5182.0
				Mg I (m2) 5183.6
				Fe II [m19F] 5184.8
5193.9	58.3	5196.0	70.6	Fe II (m49) 5197.6
5231.8	70.8	5233.8	141.2	Fe II (m49) 5234.6
5315.3	100.0	5316.0	135.3	Fe II (m49) 5316.6
				Fe II (m48) 5318.8
5363.5	37.5	5364.5	58.8	Fe II (m48) 5362.9

NOTE.—Number 1 indicates observations made on 1998 March 14; Number 2 indicates observations made on 2000 June 9.

TABLE 7  
OBSERVED EMISSION LINE INTENSITIES RELATIVE TO  $H\beta = 100$ , OBTAINED WITH CASSEGRAIN DATA.

Wavelength ( $\text{\AA}$ ) <sup>1</sup>	I( $\lambda$ ) <sup>1</sup>	Wavelength ( $\text{\AA}$ ) <sup>2</sup>	I( $\lambda$ ) <sup>2</sup>	Identification
5425.0	120.8	5424.7	229.4	Fe II (m49) 5425.3
5472.5	57.5	5473.6	81.2	Fe II [m34F] 5477.3
				Fe II (m49) 5477.7
				Cr II (m50) 5479.0
5502.0	69.2	5502.5	88.2	Cr II (m50) 5502.8
				Cr II (m50) 5503.6
				Cr II (m50) 5510.1
5530.2	79.2	5530.8	100.0	Fe II [m17F] 5527.3
				Fe II (m55) 5527.6
				Fe II [m16F] 5527.6
5565.1	26.7	5567.5	47.1	Utd
5587.2	42.1	5587.5	47.1	Fe II [m39F] 5588.2
5622.1	28.8	5623.7	38.8	Fe II (a2P-b2D) 5627.3
5640.6	33.3	5641.5	44.7	Si II (m14) 5639.5
				Fe II [m18F] 5644.0
5658.2	37.1	5660.0	58.8	Fe II (m57) 5657.8
5682.6	29.6	5679.2	76.5	N II (m3) 5676.0
				N II (m3) 5679.6
				N II (m3) 5686.2
5708.3	16.7	5709.9	23.5	N II (m3) 5710.8
5753.5	62.5	5753.7	100.0	N II [m3F] 5754.8
5875.2	445.8	5875.3	470.6	He I (m11) 5875.6
5953.0	42.1	5953.2	76.5	N II (m28) 5952.4
5978.0	25.0	5979.2	47.1	S III (m4) 5979.0
5989.8	33.3	5990.2	47.1	Fe II (m46) 5991.4
6044.2	10.8	6045.0	6.5	O II (m22) 6046.3
				O II (m22) 6046.5
6083.8	29.2	6084.6	20.6	Fe II (m46) 6084.1
6113.4	20.8	6114.3	29.4	Fe II (m46) 6113.3
6127.6	25.0	6128.7	35.3	Si II (m46) 6129.7
6147.7	54.2	6148.3	105.9	Fe II (m74) 6147.7
6238.4	162.5	6239.9	170.6	Fe II (m74) 6238.2
6316.7	46.7	6317.7	60.6	Fe II (z4D0-c4D) 6318.0
				Mg I (m23) 6318.2
6345.1	70.8	6346.6	82.4	Fe II (m74) 6345.5
				Ni II (m46) 6347.1
				Si II (m2) 6347.1
6369.5	57.9	6370.6	117.7	Fe II (m40) 6369.5
				Si II (m2) 6371.4
6383.4	42.9	6383.9	64.7	Fe II 6383.8
6406.6	45.8	6404.7	30.0	Ne II (m1) 6407.9
6414.7	37.5	6415.7	40.6	Fe II (m74) 6417.9
6432.1	42.9	6433.0	44.7	Fe II (m40) 6432.7
6454.3	54.2	6455.7	64.7	Fe II (m74) 6456.4
6488.8	72.5	6488.8	99.4	Fe II 6489.6

NOTE.—Number 1 indicates observations made on 1998 March 14; Number 2 indicates observations made on 2000 June 9.

TABLE 7  
OBSERVED EMISSION LINE INTENSITIES RELATIVE TO  $H\beta = 100$ , OBTAINED WITH CASSEGRAIN DATA.

Wavelength ( $\text{\AA}$ ) <sup>1</sup>	I( $\lambda$ ) <sup>1</sup>	Wavelength ( $\text{\AA}$ ) <sup>2</sup>	I( $\lambda$ ) <sup>2</sup>	Identification
6514.8	53.8	6515.7	61.8	Fe II (m40) 6516.1
				Fe II (m72) 6518.2
6547.4	29.2	6548.9	35.3	N II [m1F] 6548.1
6561.9	333.3	6562.5	317.7	He II (m2) 6560.1
				H $\alpha$ 6562.8
6582.9	38.3	6582.6	41.8	N II [m1F] 6583.6
6677.4	233.3	6677.9	252.9	He I (m46) 6678.2
6716.3	20.8	6718.1	11.2	S II [m2F] 6716.4
7040.4	28.3	7041.4	35.3	Al II (m3) 7042.1
7064.1	325.0	7064.2	317.7	He I (m10) 7065.2
7220.1	45.8	7220.2	35.3	Fe II 7224.5
7260.9	6.3	7260.3	19.4	N II (m52) 7259.3
7281.4	111.3	7281.9	164.7	He I (m45) 7281.4
7306.8	25.0	7305.3	52.9	Fe II (m73) 7308.0
7321.5	16.7	7319.9	47.1	O II 7319.0
				Fe II (m73) 7320.7
—	—	7417.0	64.7	N II [m2F] 7411.6
—	—	7444.7	52.9	N I (m3) 7442.3
—	—	7510.7	57.7	Fe II (m73) 7515.9

NOTE.—Number 1 indicates observations made on 1998 March 14; Number 2 indicates observations made on 2000 June 9.

TABLE 8

OBSERVED ABSORPTION LINE INTENSITIES RELATIVE TO  $H\beta = 100$ , OBTAINED WITH CASSEGRAIN DATA.

Wavelength ( $\text{\AA}$ ) <sup>1</sup>	I( $\lambda$ ) <sup>1</sup>	Wavelength ( $\text{\AA}$ ) <sup>2</sup>	I( $\lambda$ ) <sup>2</sup>	Identification
4264.9	-38.8	4265.8	-88.2	N I 4264.0
4282.7	-45.8	4287.3	-51.8	Uid
4330.7	-66.7	4332.9	-100.0	N III (m10) 4335.5
4344.7	-24.2	4346.3	-76.5	N III (m10) 4348.4
4429.6	-220.8	4428.4	-100.0	N II (m33) 4427.8
—	—	4746.4	-45.3	Uid
4879.8	-38.8	4879.6	-76.5	N III (m9) 4881.8
5673.2	-11.3	—	—	Fe II 5673.2
5737.9	-5.0	5740.2	-21.8	Si III (m4) 5739.8
6073.6	-7.5	6074.8	-7.9	He II (m8) 6074.1
6203.3	-58.3	6204.4	-26.5	Uid
6977.4	-10.4	6977.6	-47.1	Uid

NOTE.—Number 1 indicates observations made on 1998 March 14; Number 2 indicates observations made on 2000 June 9.